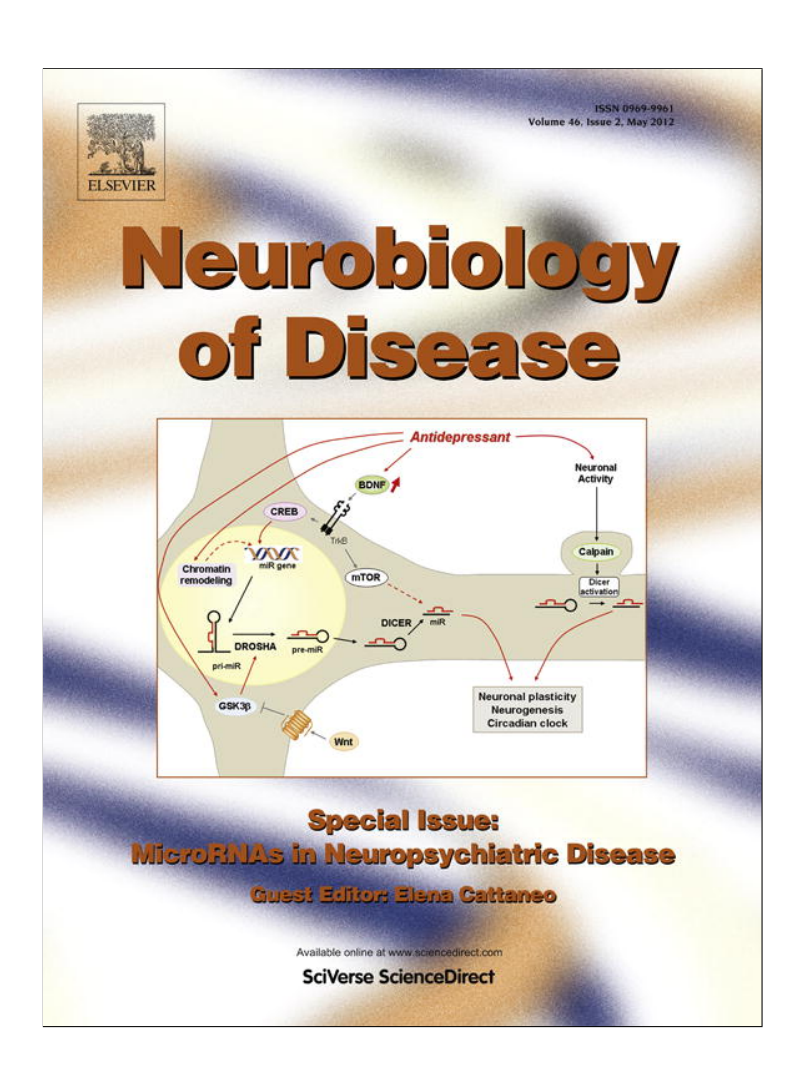
Provided for non-commercial research and education use. Not for reproduction, distribution or commercial use.



This article appeared in a journal published by Elsevier. The attached copy is furnished to the author for internal non-commercial research and education use, including for instruction at the authors institution and sharing with colleagues.

Other uses, including reproduction and distribution, or selling or licensing copies, or posting to personal, institutional or third party websites are prohibited.

In most cases authors are permitted to post their version of the article (e.g. in Word or Tex form) to their personal website or institutional repository. Authors requiring further information regarding Elsevier's archiving and manuscript policies are encouraged to visit:

http://www.elsevier.com/copyright

Author's personal copy

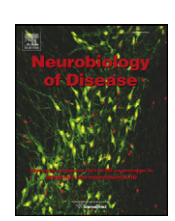
Neurobiology of Disease 46 (2012) 402-413



Contents lists available at SciVerse ScienceDirect

Neurobiology of Disease

journal homepage: www.elsevier.com/locate/ynbdi



Evolution of the dynamic properties of the cortex-basal ganglia network after dopaminergic depletion in rats

Cyril Dejean ^{a,b,c}, Agnes Nadjar ^d, Catherine Le Moine ^a, Bernard Bioulac ^{b,c}, Christian E. Gross ^{b,c}, Thomas Boraud ^{b,c,*}

- ^a CNRS, INCIA UMR 5287, F-33000 Bordeaux, France
- ^b Univ. de Bordeaux, Institut des Maladies Neurodégénératives, UMR 5293, F-33000 Bordeaux, France
- CNRS. Institut des Maladies Neurodégénératives, UMR 5293, F-33000 Bordeaux, France
- d Laboratoire de Nutrition et Neurobiologie intégrée, INRA, Université de Bordeaux, UMR1286, UFR Pharmacie 146 rue Leo Saignat, 33076 Bordeaux Cedex, France

ARTICLE INFO

Article history: Received 11 November 2011 Revised 18 January 2012 Accepted 4 February 2012 Available online 12 February 2012

Keywords: Basal ganglia Oscillations Cortex Spindles Evolution LFP Dopamine 6-OHDA Parkinson's disease Striatum Substantia nigra Electrophysiology

ABSTRACT

It is well established that parkinsonian syndrome is associated with alterations of neuronal activity temporal pattern basal ganglia (BG). An increase in synchronized oscillations has been observed in different BG nuclei in Parkinson's disease patients as well as animal models such as 6-hydroxydopamine treated rats. We recently demonstrated that this increase in oscillatory synchronization is present during high-voltage spindles (HVS) probably underpinned by the disorganization of cortex-BG interactions. Here we investigated the time course of both oscillatory and motor alterations. For that purpose we performed daily simultaneous recordings of neuronal activity in motor cortex, striatum and substantia nigra pars reticulata (SNr), before and after 6-hydroxydopamine lesion in awake rats. After a brief non-dopamine-specific desynchronization, oscillatory activity first increased during HVS followed by progressive motor impairment and the shortening of SNr activation delay. While the oscillatory firing increase reflects dopaminergic depletion, response alteration in SNr neurons is closely related to motor symptom.

© 2012 Elsevier Inc. All rights reserved.

Introduction

The basal ganglia (BG) form a complex interconnected network that processes cortical information in the frame of higher brain functions such as motor control (Graybiel et al., 1994). Numerous studies have reported temporal alterations of neuronal activity in the cortex and BG of patients with Parkinson's disease (PD) and animal models (Eusebio and Brown, 2007; Hammond et al., 2007; Hutchison et al., 2004). These are mainly abnormal bursting activity and exacerbated synchronous oscillations (Belluscio et al., 2003; Bergman et al., 1994; Sharott et al., 2005).

PD is a neurodegenerative disease and therefore has a strong evolutionary component. Because electrophysiological changes are

E-mail address: thomas.boraud@u-bordeaux2.fr (T. Boraud).

Available online on ScienceDirect (www.sciencedirect.com).

detected in patients well after the appearance of symptoms, the time of their onset remains unknown and the role of rhythmic activities in PD is still a matter of debate (Boraud et al., 2005). It is extremely difficult to address this question in patients because (1) symptoms only appear once most dopaminergic neurons have disappeared and (2) network activity rearrangements might occur during pre-symptomatic phase as shown in animal models (Day et al., 2006). Thus the specific roles of both depletion and rearrangements that derive from dopaminergic cell death remain unknown and so is the meaning of electrophysiological markers of parkinsonism such as excessive oscillatory activity. Recent clinical data indicate that oscillations could reflect responsiveness to dopaminergic treatment rather than the severity of symptoms (Weinberger et al., 2006). Moreover in a progressive primate model of PD in the monkey the appearance of oscillations is delayed compared to the appearance of the first motor symptoms (Leblois et al., 2007). 6-Hydroxydopamine (6-OHDA) intra-cerebral injection allows to quickly remove dopaminergic neurons and therefore decouples fast depletion and slower network rearrangements. With this approach we can monitor the joint evolution of symptoms and electrophysiological parameters in the

^{*} Corresponding author at: Institut des Maladies Neurodégénératives, UMR5293, F156 rue Léo Saignat, 33076 Bordeaux cedex, France.

BG. Hence, the present work aims at unraveling the co-evolution of motor symptoms and electrophysiology in the cortex–BG network after 6-OHDA lesion.

We focused on specific oscillations named high-voltage spindles (HVS) in the BG of 6-OHDA-treated rats. HVS are generated in the cortex (Polack et al., 2007) and propagate through the BG of dopamine-intact rats as well as in genetic models of absence epilepsy where their occurrence becomes prominent (Berke et al., 2004; Dejean et al., 2007; Deransart et al., 2003; Magill et al., 2005; Slaght et al., 2004; Vergnes et al., 1990). Interestingly they are further enhanced after both acute and chronic dopaminergic depletion (Dejean et al., 2008; Deransart et al., 2000). Therefore HVS represent an excellent tool to follow the changes in ability of BG neurons to sustain and increase oscillatory firing before and after 6-OHDA lesion. In the present work we recorded local field potential (LFP) and single neurons during HVS in cortex, striatum and substantia nigra pars reticulata (SNr) in freely moving animals before and during the 30 days that followed 6-OHDA treatment. To complement electrophysiology we also monitored the time courses of midbrain dopamine cell death and motor impairment related to the lesion.

Materials and methods

Animals

Male Wistar rats (350–400 g, Depré, Saint Doulchard, France) were kept under standard housing conditions at constant temperature (22 +/- 1 °C), humidity (relative, 30%), and 12-hour light/dark cycles (daylight period 08:00–20:00). Water and food were available ad libitum. Animal care and surgery were consistent with the National Institute of Health *Guide for the Care and Use of Laboratory Animals* as well as the European community council directive of November 24, 1986 (86/609/EEC) and was approved by the Comité Ethique de la Région Aquitaine.

Three subsets of animals were used in the present study. The first subset of animals called the electrophysiology group (group E) entered freely-moving electrophysiology and behavior experiment (n=4). Note that this group and some data derived from it entered a previous study (Dejean et al., 2008). A second subset (n=6) was designed to asses the effect of a sham lesion on behavior (group S). The third group (group K) was aimed at monitoring kinetics of dopamine cell loss and microglial activation (n=84).

Head-stage

A custom headstage was designed for the purposes of this experiment, to perform simultaneous recordings from the motor cortex (AnteroPosterior +1.2 to +2.2 mm, MedioLateral: 1.5 to 2.5 mm, Depth: 1.5 to 2.5 mm), the dorsal striatum (AP: +0.5 to -0.5 mm, ML: 3 to 4 mm, D: 3.5 to 5 mm) and the SNr (AD: -5.3 to -5.8 mm, ML: 1.8 to 2.7 mm, D: 7.5 to 8.5 mm). Details of the device's design and the implantation surgery can be found in a previous publication (Dejean et al., 2007). To enable the required lesion of midbrain dopaminergic neurons to be carried out, the head-stage was equipped with a 28 gauge stainless steel cannula guide (Plastic One, Roanoke, VA, USA). According to a stereotaxic atlas (Paxinos and Watson, 1998) the guide was placed directly above the medial forebrain bundle which contains the nigrostriatal dopaminergic fibers (-2.8 mm anteroposterior and + 2 mm mediolateral). The cannula length was adjusted so that once it had been inserted into the guide, its tip was positioned in the upper third of the medial forebrain bundle (depth $-8.4 \,\mathrm{mm}$). The lesioning procedure is described below.

Electrode implantation surgery

The 10 rats of groups E and S were operated under xylazine (60 mg/kg i.p. Rompun, Bayer, Germany) and ketamine (100 mg/kg i.p., Virbac, Carros, France) anesthesia. Using a stereotaxic frame (Kopf) recording targets were located, above which holes were drilled in the skull. The head-stage was lowered and the holes were filled with vaseline (Vaseline, Gifrer Barbezat, Decines, France). The head-stage was then attached to the animal's skull with glue (Superbond, Sun Medical Co., Japan), dental cement (DentalonPlus, Heraeus Kulzer, Hanau, Germany) and stainless steel screws. Note that group S animals with a cannula and a head piece similar to that of group E at the exception of the recording electrodes that where not needed in this group. Before the end of anesthesia, group E electrophysiological activities were recorded in order to make fine adjustments of the electrode positions when recorded signals did not agree with the characteristics of the targeted structures, given that the shape of action potentials is not affected by general anesthesia as shown for instance in the SNr (Windels and Kiyatkin, 2006). The animals were given ketoprofen (Ketofen 2 mg/kg, s.c., Merial, Lyon, France) following surgery, then again 24 h later for pain relief and were then allowed to recover for 7 days before the first recording session.

Electrophysiological data acquisition

Daily recordings ran for 1 h in a circular arena (40 cm diameter) during which physiological and behavioral activities were simultaneously recorded. Neural signals were pre-amplified 25 times (Mini-HeadStage, AlphaOmega Engineering, Nazareth Illit, Israel) and then amplified by a multichannel processor and digitized at a rate of 50 kHz (MCP, AlphaOmega Engineering). The raw signal was stored for further analysis at a lower rate of 12.5 kHz (AlphaMAP, AlphaOmega Engineering). In parallel, it was filtered (300 Hz-3 kHz) for online spike discrimination using a template matching procedure (Multi Spike Discriminator, AlphaOmega engineering). Discriminated spikes were stored synchronously with the raw signals. The animal's movements were recorded simultaneously by a video tracking system (VTS, Plexon Inc., TX, USA). Their position and the video recording were sampled at 30 Hz and stored separately from the neural data using video capture software (Cineplex, Plexon Inc.). Neural and behavioral signal recordings were triggered simultaneously, and the exact time of each position and video frame was sent to the Alpha-MAP and stored in the neural data files for offline synchronization.

At the end of the animals' recovery period, following surgical implantation of the head-stages, recordings were made under normal conditions for two weeks. The nigrostriatal fibers were then lesioned (see below) and recordings were resumed after 24 h under the same conditions for a period of 30 days.

6-OHDA lesion procedure

One hour before 6-OHDA injection, animals were pre-treated with intraperitoneal injections of desipramine (0.4% solution, 25 mg/kg, Sigma-Aldrich France, Lyon) and pargyline (0.1% solution, 5 mg/kg, Sigma-Aldrich France, Lyon). Desipramine is used to protect the noradrenaline neurons from 6-OHDA and Pargyline potentiates the efficacy of 6-OHDA by inhibiting monoamine oxidase (Dunnett, 1983).

Groups E and S

The animals were anesthetized with isoflurane gas (induction at 4% then 2%) for the duration of the injection. The injection needle was inserted through the guide mounted on the head stage (see above), and a Hamilton syringe was used to inject 6-OHDA (Sigma-Aldrich France, Lyon) or saline (1 μ L) into the medial forebrain bundle (see above). A total of 8 μ g of 6-OHDA was injected in 1 μ L of saline solution containing ascorbic acid 1 mM at a rate of 0.5 μ L/min. After

the injection had been completed, the syringe was left in place for 5 additional minutes in order to prevent the liquid from flowing back up the guide.

Group K

Rats were anesthetized with ketamine hydrochloride (75 mg/kg, i.p.) and xylazine hydrochloride (10 mg/kg, i.p.). Animals were fixed on a stereotaxic frame and spatial coordinates of medial forebrain bundle were defined before holes were drilled in the skull above that location. Injection device was then lowered in the brain and 6-OHDA (8 μ g) was injected into the medial forebrain bundle. Half of the rats were injected with the same volume of vehicle solution (saline 0.9%).

Histology

Tissue processing

For group E, following the final recording, the rats were given a lethal dose of pentobarbital (Pentobarbital Sodique, CEVA, Libourne, France). Immediately after the injection, electrical microlesions (30 μ A, 10 s) were induced by passing an anodal current through one electrode at each recording site. The brain was then quickly removed and frozen in an isopentane bath at $-80\,^{\circ}\text{C}$ for histological analysis. Coronal brain sections (20 μ m) were cut and those encompassing the motor cortex, striatum and SNr were mounted on slices

for electrode placement verifications. These slices were stained with cresyl violet for brain structure identification. The recording tracks and sites were then established by observing the marks left by the cannulas and electrolesions (Fig. 1A).

For group K, at day 0, 3, 8, 13, 18, 23 or 28 post-intoxication, rats were an esthetized with urethane. After perfusion with 0.9% NaCl followed by 4% paraformal dehyde (PFA), brains were removed, post-fixed in the same fixative for 1 night at 4 °C, immersed in 20% sucrose, frozen by slow immersion in isopentane, cooled on dry ice at $-45\,^{\circ}\mathrm{C}$, and stored at $-80\,^{\circ}\mathrm{C}$ before sectioning. We used a cryostat at $-19\,^{\circ}\mathrm{C}$ to cut 30 $\mu\mathrm{m}$ coronal sections, which were collected free floating for immunohistochemistry.

Optical density of striatal dopamine transporter

In group E animals the passage of microelectrodes through the SNc on their way to the SNr prevents from any accurate cell count in the dopaminergic structure. However the extent of the SNc lesion can be determined by measuring the amount of dopamine cell terminals remaining in the striatum ipsilateral to the lesion compared to the contralateral side (Kunikowska and Jenner, 2001). Dopamine transporters are present at the membrane of nigrostriatal dopamine cell terminals and give a indirect measure of the amount of SNc dopaminergic cells projecting to the striatum. Dopamine transporter binding procedure was performed as described previously (Bezard et al., 2001). After purification, [125I](E)-N-(3-iodoprop-2-enyl)-2β-

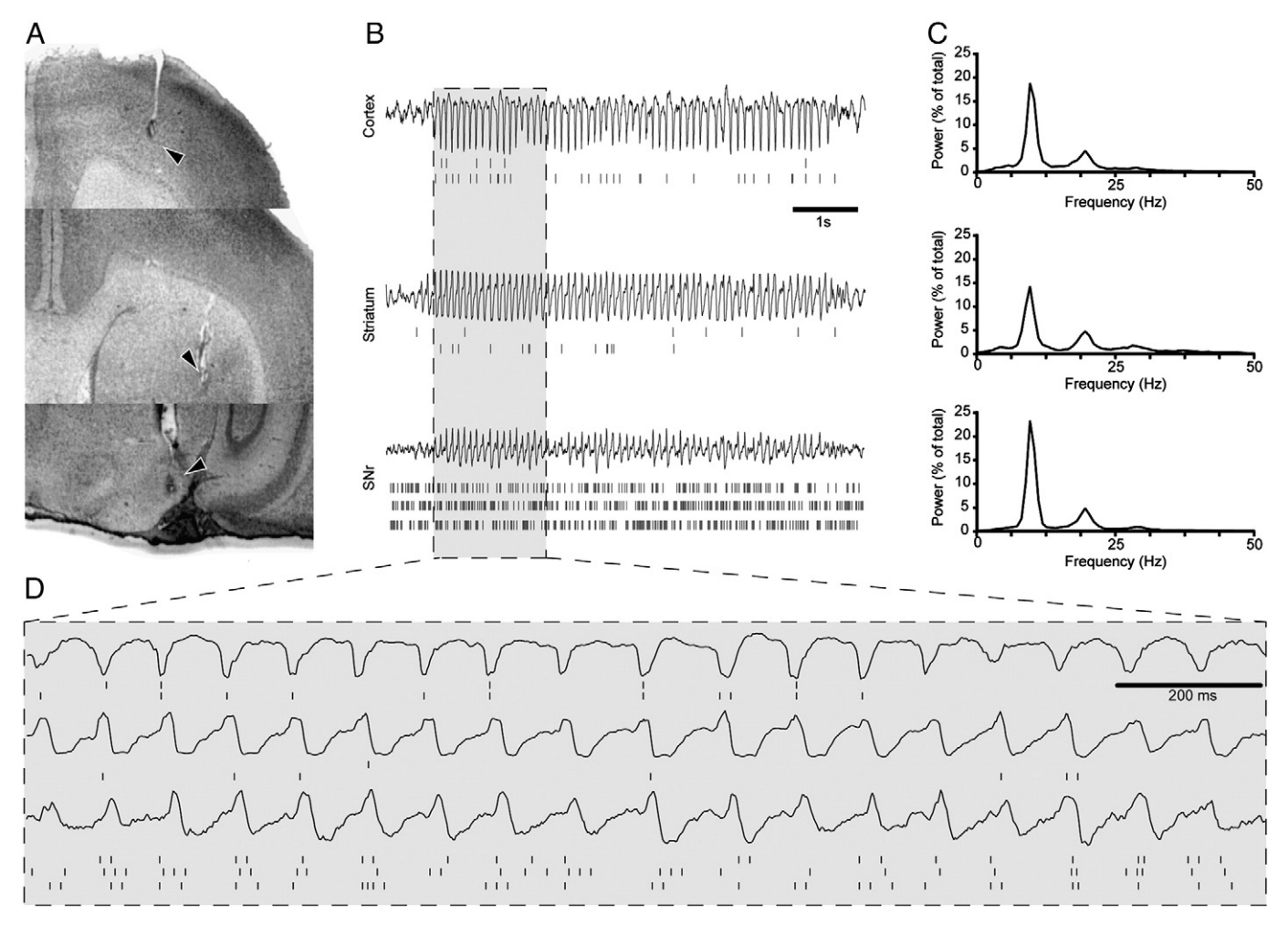


Fig. 1. Recordings sites. A. Coronal sections stained with cresyl violet at the level of recording sites in motor cortex (up), striatum (center) and SNr (bottom). Arrowheads show electrolytic microlesion locations. All slices have been taken from the same rat (rat #2). B. Electrophysiological activities simultaneously recorded in motor cortex (up), striatum (center) and SNr (bottom) in rat #2. Lines represent the local field potential. Below, the vertical bars represent the spike trains of simultaneously recorded single neurons (2 in cortex, 2 in striatum and 3 in the SNr). C. Power spectrum of the LFP displayed in B shows a peak in the 8–12 Hz range. D. Magnification of the portion of B panel shown within the dotted line box.

carboxymethyl- 3β -(4'-methylphenyl) nortropane (PE2I) was obtained in a no-carrier-added form with a specific activity of 2000 Ci/mmol and stored in ethanol at $-20\,^{\circ}$ C, a temperature at which it remains stable for 1 month. Sections were incubated for 90 min at 25 °C with 100 pM [125I] PE2I in pH 7.4 phosphate buffer (in mM: 10.14 Nah2PO4, 137 NaCl, 2.7 KCl, and 1.76 KH₂PO₄). After incubation, all sections were then washed twice for 20 min in phosphate buffer at 4 °C and dried at room temperature. They were then exposed to β -radiation-sensitive film (Hyperfilm β -max; GE Healthcare, Buckinghamshire, UK) in X-ray cassettes, for 7 d, for autoradiographic assessment of the radioactivity bound to regions of interest. The optical density was measured on 4 different sections per animal with an image analysis system (Densirag V. D2.00; Biocom, Les Ulis, France) and averaged for each right and left striatum in each animal.

TH immunohistochemistry

Serum containing TH antibody (polyclonal rabbit TH antibody, J. Boy, Reims, France) was diluted 1:2000 in phosphate-buffered saline (PBS) containing 0.3% Triton X-100 and 1% bovine serum albumin (BSA), and sections were incubated overnight at 4 °C, before being incubated for 2 h with biotinylated horse anti-rabbit antibody (universal secondary antibody, AbCys SA, Paris, France) diluted 1:500 in PBS/1% BSA/0.3% Triton X-100, for 2 h with avidin–biotin peroxidase diluted 1:200 in PBS (Vectastain ABC kit; Vector Laboratories, Burlingame, CA), and finally revealed with 3,3'-diaminobenzidine tetrahydrochloride (DAB kit, Vector Laboratories). Sections were then slidemounted and counterstained with cresyl violet.

Counting of TH-immunoreactive (TH+) neurons

Brain sections were examined under light microscopy using an image analysis system (Mercator; Explora Nova, La Rochelle, France). Four sections per animal were analyzed by an examiner blind to experimental conditions. Structure considered was the SNc. An optical dissector probe was used to count the cells per mm² for each brain region per animal at a 40× magnification. Dissectors (length 50 μm , width 40 μm) were separated from each other by 30 μm (x) and 20 μm (y). In these dissectors, the nuclei of the neurons were counted into focus. A neuron was counted in the whole slice thickness, only if more than half the cell was inside the two consecutive boundaries taken into account. Mean cell number per plane and SEM were then calculated for each group of rats.

Behavioral analysis

Offline discrimination of movement and rest episodes was carried out using Cineplex Markup software (Plexon Inc., Littleton, MA, USA). The choice of the motor parameter to measure in order to asses the impact of the lesion on the animal behavior was done in favor of locomotor activity. Locomotor activity has been shown recently to be decreased in rats bearing unilateral dopaminergic lesion (Kravitz et al., 2010; Steiner and Kitai, 2001). Self induced locomotor activity fits one important constraint of this study, to record physiological parameters in the unrestrained animal. For that reason we ruled out both the stepping test (Olsson et al., 1995) and drug-induced rotation tests.

Movement episodes consisted in periods during which the animal was moving (with the exception of grooming and rearing episodes, see below). Basal locomotor activity was characterized by the animal's average speed and SD (cm/s). A threshold was then defined as the upper confidence limit of the mean (see Statistical analyses section). The animal was considered to be active when its instantaneous speed exceeded this threshold for > 0.5 s. Rearing and grooming episodes were sorted manually using Cineplex Markup. The animals' locomotor activity was influenced by habituation to the environment. As expected the prominent exploratory behavior observed during the first exposures of the animal to the recording chamber was

decreased after a few days of habituation. To avoid confusion between the effect of lesion and habituation on locomotor activity the present study only considered data collected after the habituation phase for the behavioral analysis. Because of the high incidence of mechanical artifacts in electrophysiological recordings grooming episodes were automatically excluded by offline joint analysis of behavior and electrophysiological traces. Rearing was present during the first days of the control period but quickly disappeared, as the animal became accustomed to the recording chamber. For these reasons, rearing data is not discussed in the present paper.

Analysis of the animals' specific behavioral patterns during HVS episodes revealed that they were awake and resting quietly, while remaining responsive to tactile, auditory and visual stimuli. Neither whisker twitching movements nor tremors were observed during HVS and this was true before as well as after the lesion of midbrain dopaminergic cells.

Signal processing

Spike sorting

The striatum contains several types of neuron, among which the medium spiny cells are the only output neurons. In this study, only putative MSNs (Medium Spiny Neurons) discriminated according to shape and frequency criteria are described. Cells with a mean hyperpolarization duration greater than 300 μs and a firing rate less than were classified as MSNs (adapted from Berke et al., 2004). Cells with a mean valley duration less than 300 μs and a firing rate greater than 1 spike/s were classified as putative interneuron. Cells not satisfying one of these two conditions were rejected. Very few interneurons (n=3) were recorded during this study. As a consequence, results related to them are not presented here. All striatal neurons with waveform valleys less than 300 μs and mean discharge rates under 1 spike/s were rejected.

At depth 1.5 to 2.5 mm at which cortical neurons have been recorded in the present study the tissue contains interneurons and pyramidal neurons (not necessarily sending axons in the pyramidal tract). Both types were discriminated using waveform timing criterion (Bartho et al., 2004). Cells presenting a peak-valley duration larger than 500 μ s were classified as putative pyramidal neurons (n = 120). Other cells were classified as putative interneurons (n=3). Only pyramidal projection neurons were considered in this study. Corticostriatal neurons only represent a subset of projection neurons. The setup and recording procedure described here does not allow connectivity tests to be performed, such as antidromic stimulation or marker tracing, in order to detect whether neurons were actually sending axons to the striatum. It was assumed that part of the recorded cortical neurons were putative corticostriatal neurons. Moreover, simultaneous multiple single-unit recordings showed that projecting neurons (thus including corticostriatal) fire synchronously in a short time window during HVS (Kandel and Buzsáki, 1997). Therefore, in our recordings the overall firing time of cortical neurons is likely to be representative of the corticostriatal population itself.

The SNr contains a majority GABAergic neurons generating brief action potentials at a sustained firing rate and a few dopaminergic neurons which when recorded extracellularly have been described as firing polyphasic long action potentials > 1.5 ms at a slow rate < 8 Hz (Hyland et al., 2002). Here the entire population of recorded neurons (n = 153) presented short biphasic extracellular action potentials (ranging from 0.81 to 1.14 ms). Thus they entered the study considered as putative GABAergic projection neurons.

HVS discrimination

HVSs exhibit two main features, namely a spike and wave pattern and an oscillation frequency ranging between 5 and 13 Hz (Figs. 1B, C and D). Power spectrum histograms display a second peak in the beta range (15–30 Hz, Fig. 1C). A careful inspection of raw traces during

HVS episodes did not reveal any prominent beta oscillations. Therefore the observed peak in the beta range may therefore represent harmonics of the fundamental 5-13 Hz frequency. Because this induces an analytic bias, we could not further take into account the beta band in the present paper. Both pattern and frequency criteria were used to detect the onset and offset of HVS. For frequency criteria, a threshold on the instantaneous power spectral density (PSD) of LFP was used. LFP were first filtered (1-200 Hz) using a 2nd order band-pass Butterworth filter, and then down-sampled (500 Hz). For each structure, the PSD was computed every 100 ms using an overlapping sliding window with a length of 250 points (0.5 s). The instantaneous averaged PSD in the 5-13 Hz range was computed for each time step. Its value was deemed to be significantly increased when it passed the confidence limit (see Statistical analyses section). Over-threshold time steps determined preliminary epochs. A pattern criterion was assessed manually. Preliminary epochs, within which the LFPs showed no typical spike and wave pattern, were rejected. Previous studies showed that HVS onset and offset could occasionally be different in cortex and striatum (Berke et al., 2004). This lag can be attributed to the fact that onset and offset may vary across cortical locations (Polack et al., 2007; Shaw, 2004). Since the cortical recording electrode was placed at a given location, the HVS could have been transmitted first from another cortical location to the striatum, thereby introducing an apparent onset delay. The same phenomenon could account for a delay in observed offsets. The analysis time frame was restricted to oscillation cycles, where all three structures were oscillating. To remove the lag-related bias, only those time intervals having overlapping candidate epochs were taken into account, using Neuroexplorer software (Nex Technologies, MA, Littleton, USA).

HVS oscillation trough and peak markers were then discriminated within HVS epochs using temporal and voltage criteria with a homemade routine running under Matlab (The Mathworks, Natwick MA, USA). Cortical electrodes were placed around the border of layer V and VI (~1.5 to 2.5 mm below the surface) to record projection neurons. At this level, the earliest HVS spike component is negative (Kandel and Buzsáki, 1997). For this reason, cortical LFP markers were positioned at the minimum voltage in the troughs. As striatum and SNr spike components are positive, striatal and nigral markers were positioned at the maximum voltage in the peaks.

Spectral characterization of LFP

The power spectral densities of LFPs were computed using Fast Fourier Transform (FFT) analysis, and Welch method as spectral estimator with a sliding windows of 1250 samples (2.5 s), over the frequency range from 0 to 500 Hz (0.39 Hz resolution). Histograms were smoothed using a three-point Gaussian process.

Coherence was computed using the expression:

$$\textit{Coherence}_{ij} = \left(P_{ij} \times P_{ji}\right) / \left(P_{ii} \times P_{jj}\right)$$

where P is the average of the squares of the LFP spectra i and j. These spectra were computed using the same method as described above (unless otherwise stated).

Characterization of spike trains

Cross-correlograms were computed with bin size = 2 ms and a minimum number of 50 reference spikes. Power spectral densities of cross-correlograms were computed by Fast Fourier Transform analysis using sliding windows of 256 samples (1.25 s) in the range 0–200 Hz, yielding a resolution of 0.8 Hz. Histograms were smoothed with a three-point Gaussian window. The confidence limits of power spectral density histograms were computed in the 3–50 Hz range (see Statistical analyses section) and autocorrelograms and cross-correlograms were considered significantly oscillatory if any power

spectral density value in the range 5–13 Hz passed the confidence limits

Time lag distributions

Peri-event histograms of the discharge activity of single neurons and of the next cortical LFP markers were constructed, using the HVS cortical marker as a trigger (t_0), over a time frame of 100 ms before and after t_0 . For the purposes of graphical representation, a 2 ms bin size and a three-point Gaussian smoothing algorithm were used. For this analysis only triggers and spike trains which occurred more than 50 times in the HVS epochs were considered. A peak was considered significant if it exceeded the upper confidence limit (see Statistical analyses section), and a trough was considered significant if its value was below the lower confidence limit. The presence of a significant peak and/or trough was used as a criterion in defining a neuron to be "HVS driven". For the HVS driven neurons, peak and trough times were averaged in order to construct population time lag distributions in the time range of 50 ms before and 140 ms after cortical LFP marker.

Phase relationship

To determine the phase relationship between neurons and cortical LFPs following the method used by Klausberger et al. (2003) we used a Matlab algorithm (see HVS discrimination section) to detect the troughs of HVS. Each spike was assigned to a phase between the troughs n and n+1 given that the peak of LFPs was arbitrarily assigned the angle value 0°. The circular space was divided into 100 bins of equal size giving a resolution of 3.6°. The significance of the phase relationship was analyzed using the Rayleigh test for directional data (Fisher, 1993). This tests the hypothesis that spike phases are uniformly distributed along the circular space (0-360°). For each spike train this test was carried on 50 randomly chosen action potentials to test samples of the same size and avoid analytic bias related to differences in sample size. The preferred phase (i.e. phase represented by the highest number of spikes) was collected to build the phase distributions for neurons. This phase analysis of neuronal spike trains revealed that the neurons that presented a significant bias toward a preferred phase of cortical LFPs were also the ones that were defined as 'HVS driven' by the time lag analysis (previous section). This shows that firing rate of neurons selected for this study had no influence on their oscillatory behavior.

$Statistical\ analyses$

Statistical analyses were performed with the Sigma Stat software (Version 2.03; SPSS Inc, Chicago, IL, USA) and GraphPad Prism (version 4.00, GraphPad Software, San Diego CA, USA). A probability level of 5% (p<0.05) was considered significant. Variables are presented in the following form: mean \pm SEM. Time was discretized into the following time periods: the control (ctrl) interval that covers pre-6-OHDA period, and post lesions day intervals [0–5], [5–10], [10–15], [15–20], [20–25] and [25–30].

Confidence limits were computed as CL = mean ± 3SD. Comparisons between locomotor activity during each time interval were made using a Kruskal–Wallis test followed by post-hoc Dunn's test. Influence of the lesion on HVS duration, HVS number, coherence and LFP oscillation frequencies were equally assessed using a one way ANOVA followed by post-hoc Bonferroni test. Oscillatory AC and CC percentages were analyzed using chi-square tests (ctrl vs. post-lesion intervals). Auto and crosscorrelograms percentages inside and outside HVS period were compared using a one-way ANOVA. Firing rates inside and outside HVS episodes were compared using a Kruskal–Wallis test. AC mean oscillation frequencies were compared using a one-way ANOVA followed by post-hoc Bonferroni test (ctrl vs. various intervals). Firing rates were analyzed with a Kruskal–Wallis test followed by post-hoc Dunn's test. Time lags between neuron

firing peaks and LFP peaks presented non-normal distributions and unequal variances. They were therefore analyzed using Kruskal–Wallis test followed by post-hoc Dunn's test. The comparison of phase distributions in the circular space for control and lesion condition was done using the Watson U2 test (Fisher, 1993). For TH+ and weight loss analysis, a two-way repeated measure ANOVA was applied followed by *post hoc* Tukey's tests.

Locomotor activity is expressed as a percentage of the time spent moving under control conditions. ACs and CCs are presented as a percentage of the total AC and CC, respectively.

Results

Motor impairments follow 6-OHDA lesion

The effect and kinetics of the lesion on spontaneous locomotion were assessed in groups E and S (Fig. 2). In the control period the time spent moving averaged 20.6 ± 0.76 and 19.83 ± 1.71 in groups E and S respectively. In group S lesion didn't have any effect on spontaneous locomotion (Kruskal-Wallis test, p = 0.9086). In group E between 0 and 5 days post lesion, locomotion was strongly decreased compared to group S (4.26 ± 1.10 , Kruskal-Wallis test, p<0.05; post-hoc Dunn's test, p<0.001). Interestingly during this period animals displayed abnormal signs of distress such as a hunched posture and piloerection that were not observed in saline treated rats. However both distress signs and locomotor impairment were only transient and restricted to [0-5] period. Time spent moving reached back control level at days [5-10] and [10-15] post lesion (post-hoc Dunn's test, p>0.05 in each case). From 15 days post lesion however, locomotor activity durably and significantly dropped at around half of its control level for periods [15-20], [20-25] and [25-30] with values respectively reaching $8.9\% \pm 2.6$, $8.8\% \pm 2.5$ and $9.7\% \pm 3.7$ (Kruskal-Wallis test, post-hoc Dunn's test, p<0.001 in each case). No difference was observed between rats within each of the two groups (two way ANOVA, Factor A: rat, p = 0.18; Factor B: ctrl/lesion, p < 0.05).

Dopaminergic depletion and kinetics of neuronal loss within the SNc

In group E the extent of the damage to dopaminergic neurons subsequent to the lesion was assessed by a measure of dopaminergic terminal density in the striatum. This test revealed that in the striatum ipsilateral to the lesion optical density was decreased by an average of $78.2\pm6.9\%$ compared to contralateral side (Fig. 3A). This confirmed that injection of 6-OHDA in this group resulted in a severe lesion of dopaminergic cells.

In group K neuron loss was assessed by counting and comparing the number of dopaminergic neurons in the lesion and non-lesioned

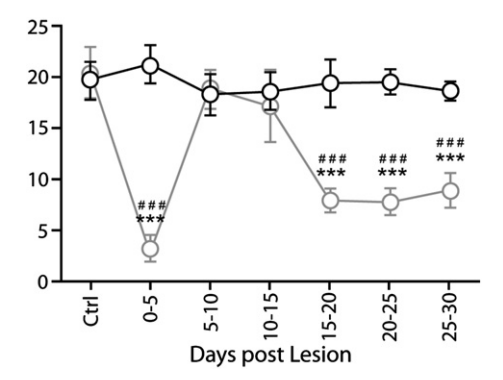


Fig. 2. Time course of motor behavior impairment after nigrostriatal lesion. Percentage of time spent moving averaged across time steps in 6-OHDA (gray) and sham lesion groups (black). Error bars: SEM. Asterisk and hash indicate a significant difference from control and sham condition respectively (Kruskal–Wallis one way ANOVA on ranks followed by a Dunn's *post hoc*, p<0.001).

SNc (Figs. 3B and C). For period [0-5], number of TH+ cells was not significantly decreased within the SNc, compared to control (21.6% loss; one-way ANOVA; p>0.05 for [0-5] versus control). Thus, the concomitant decrease of motor behavior was not related to dopaminergic neuron loss. Reciprocally, as soon as 8 days after 6-OHDA treatment, rats had 82% less dopaminergic neurons in the injected side than in the contralateral side of the SNc. The difference in the number of TH+ neurons between both side was statistically significant (one-way ANOVA followed by post-hoc Tukey's test, p<0.05 for both [5-10] versus control and [5-10] versus [0-5]). At 28 days post-treatment we observed a severe neuronal loss with an 86.2% ratio (one-way ANOVA followed by post-hoc Tukey's test, p<0.05 for both [25-30] versus [control] and [25-30] versus [0-5]).

To verify that 6-OHDA neurotoxic effects were not a consequence of an injection-induced mechanical injury, we quantified the number of TH+ neurons within the SNc of saline-treated animals. As anticipated, we found that the number of TH+ neurons in the injected side was not statistically different from the non-injected side in sham animals.

Evolution of the HVS feature after dopaminergic depletion

In the LFP of the 4 rats that entered group E, HVS characteristically recorded in control conditions had an occurrence rate of 52 ± 8.247 times in an hour, lasting 1.5 ± 0.1 s on average with an average frequency of 8.8 ± 0.4 Hz in the 5–13 Hz range (Figs. 4A–E). Those spindles were simultaneously observed in the LFPs of motor cortex, striatum and SNr. Synchronization level between those structures as quantified by coherence in the 5–13 Hz band was on average of 0.47 ± 0.03 between cortex and striatum, 0.3 ± 0.04 for cortex and SNr and 0.46 ± 0.03 for striatum and SNr (Figs. 4F–H).

In parkinsonian conditions HVS oscillation frequency remained constant (Figs. 4C–F) as well as the spike and wave pattern that usually characterize them. This is an indication that the very mechanisms underpinning HVS generation were preserved in our animals despite the lack of dopamine in the system. Nonetheless dopamine depletion had a profound impact on synchronization through the BG. Immediate effects ([0–5]) following 6-OHDA injection comprised a dramatic decrease in the length and number of HVS (Figs. 4A–B, one-way ANOVA, post-hoc test Bonferroni p<0.05 in both cases) along with a strong drop in coherence (Figs. 4F–H) between cortex–striatum as well as cortex–SNr in the 5 and 13 Hz range (one-way ANOVA, post-hoc test Bonferroni p<0.05 in both cases). This drop is not seen in group statistics for striatum–SNr while two animals showed a strong decrease the other two did not show any marked change.

These early changes in the 5–13 Hz range synchronization disappear and even reverse later in the experiment. First both the duration and number of HVS increased significantly in the [10–15] period and maintained significantly higher values during [15–20], [20–25] and [25–30] (one-way ANOVA, post-hoc Bonferroni test p<0.05 for each period). The coherence values (Figs. 4F–H) were also found significantly increased as early as [5–10] in cortex–striatum, striatum–SNr and cortex–SNr pairs and remained above control level until the final recording period [25–30] (one-way ANOVA, post-hoc Bonferroni test p<0.05 in all cases).

Dopaminergic depletion causes a time-dependent enhancement of single neuron oscillations

The single neurons we recorded during HVS in control condition (example waveforms in Fig. 5A) displayed average firing rates such as 3.8 ± 1.4 spikes/s in cortex, 0.87 ± 0.17 in striatum and 21.0 ± 2.9 in the SNr (Fig. 5D). No significant changes were observed between HVS episodes and other epochs of our recordings (paired *t*-test: $p\!=\!0.976$, $p\!=\!0.759$ and $p\!=\!0.489$ respectively). During HVS in normal conditions the average oscillation frequency observed in neuron

C. Dejean et al. / Neurobiology of Disease 46 (2012) 402-413

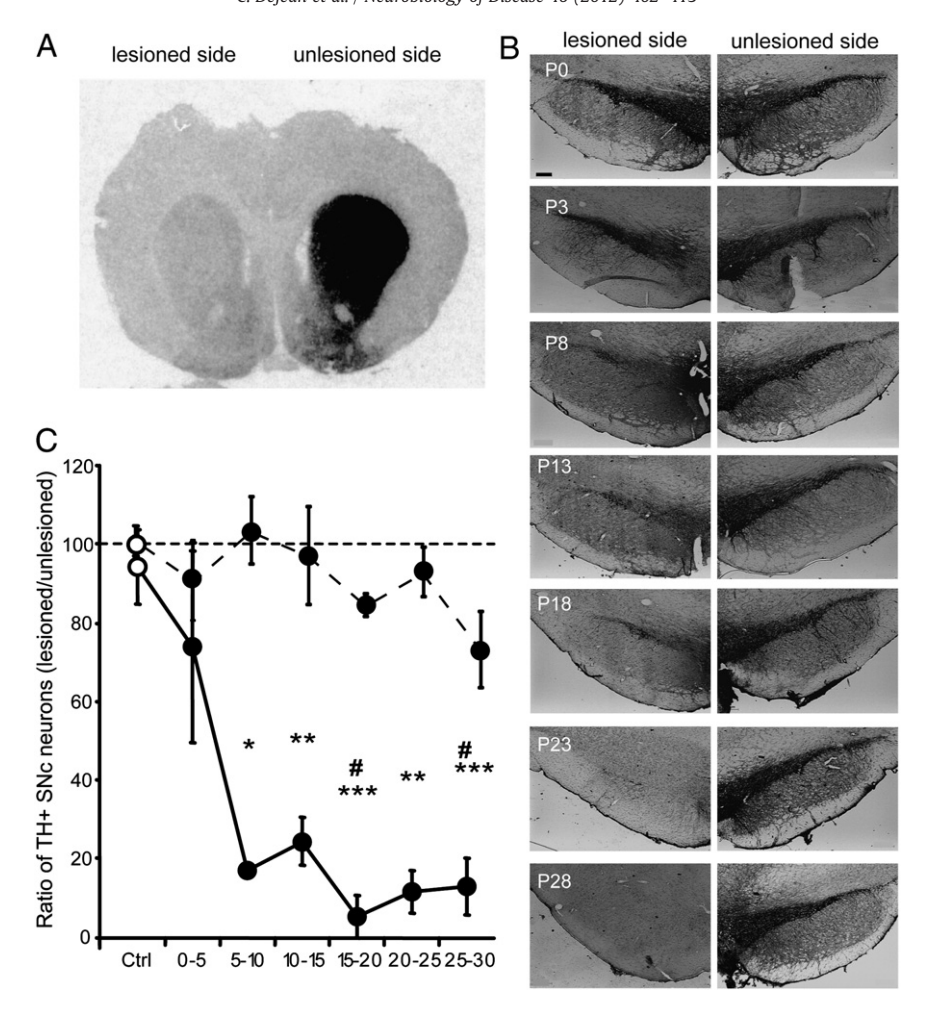


Fig. 3. Surgical protocol commonly used to induce dopaminergic loss is paralleled by the development of a sickness behavior on the first days post-intoxication. A. Density of dopaminergic terminals in the striatum after unilateral 6-OHDA administration within the medial forebrain bundle. This animal from group E presents a severe loss of labeling in the lesioned side. B. Kinetic of dopaminergic neuron degeneration after toxin injection in group K. While the unlesioned side stays intact from day 0 to day 28 post-lesion (P0 and P28 respectively). C. Quantitative analysis of TH+ neurons reveals a significant decrease of the number of dopaminergic neurons from period [5–10] post treatment. TH+ neurons then kept decreasing until [25–30]. Saline injected animals do not show any significant change (2-way ANOVA, day and treatment as factors, followed by a post-hoc Tukey test). We found a day effect: p<0.001 and a subject effect (p<0.001) as well as an interaction between factors (p=0.007) (* comparison to J0, # comparison to J3).

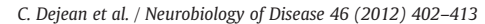
autocorrelograms ranged from 6 to 13 Hz (Figs. 5B, C and F) and did not significantly differ from that observed in LFP (t-test: 9.5 ± 0.3 Hz with a range of 6.1 to 11.4, p = 0.209). Neuronal activity reflected oscillatory activity seen in the LFP with 50.0% of cells in the cortex displaying oscillatory autocorrelograms, as well as 27.3% in striatum and 55.0% in the SNr (Figs. 5B, C and E). Single neurons from one structure to another also displayed synchronized oscillations when the LFPs showed high levels of coherence. This was evidenced by analyzing crosscorrelograms that showed significant oscillations in 21.9% of cortex–striatum pairs of neurons, 51.0% of striatum–SNr pairs and 53.8% for cortex–SNr pairs (Figs. 5B, C and E). The proportion of oscillatory auto and crosscorrelograms was significantly higher during HVS than during the rest of the recording period where the percentage of significant oscillatory neurons hardly reached 5% (one way ANOVA: p < 0.05, data not shown).

Following 6-OHDA intracranial injection, neuronal firing rates dropped significantly in the cortex and the SNr for time interval [0-5] (Kruskal–Wallis test, p<0.05, post-hoc Dunn's test, p<0.05 for both samples) but remained similar to control condition for every other period (Kruskal–Wallis test, p<0.05, post-hoc Dunn's test, p>0.05). Firing rate of striatal neurons increased progressively with periods [10-15] and [20-25] being significant compared to control. Moreover no significant changes in firing rates were observed between HVS and other epochs of our recordings (one way ANOVAs: p>0.05 in all epochs post lesion). While changes in firing rates

have been reported especially in the striatum of 6-OHDA treated rats (Kish et al., 1999; Chen et al., 2001), the moderate or lack of alteration here could be explained by a slightly lower extent of the lesion (80% compared to >90% in other studies) but it has also been suggested that the combined inhibition of direct pathway MSNs and disinhibition of indirect pathway MSNs has a net effect on global firing rate that is null (Mallet et al., 2006). The percentage of oscillatory autocorrelograms was significantly increased from [5-10] in each of the neuronal populations considered (Figs. 5B and E, chi-square test, white asterisks indicate p<0.05). Moreover the percentage of oscillatory crosscorrelograms, as well as cortical and striatal autocorrelograms was significantly increased from [10-15] but also kept increasing until the end of the experiment as shown by the significant difference between [10-15] and the final period [25-30] (Figs. 5B and E, chi-square test, hash sign indicates p<0.05). Note the average value of autocorrelogram oscillation frequency (Figs. 5C and F) did not significantly differ from that in normal condition (one-way ANOVA: p>0.05 for each structure). Moreover, no significant differences were observed between oscillation frequency in neurons and that in LFP (Fig. 5F, one-way ANOVA, p > 0.05 for each structure).

Evolution of spiking temporal organization after dopamine depletion

In control condition the majority of neurons were time-locked on HVS. When triggered by LFP peaks in the cortex where HVS originate,



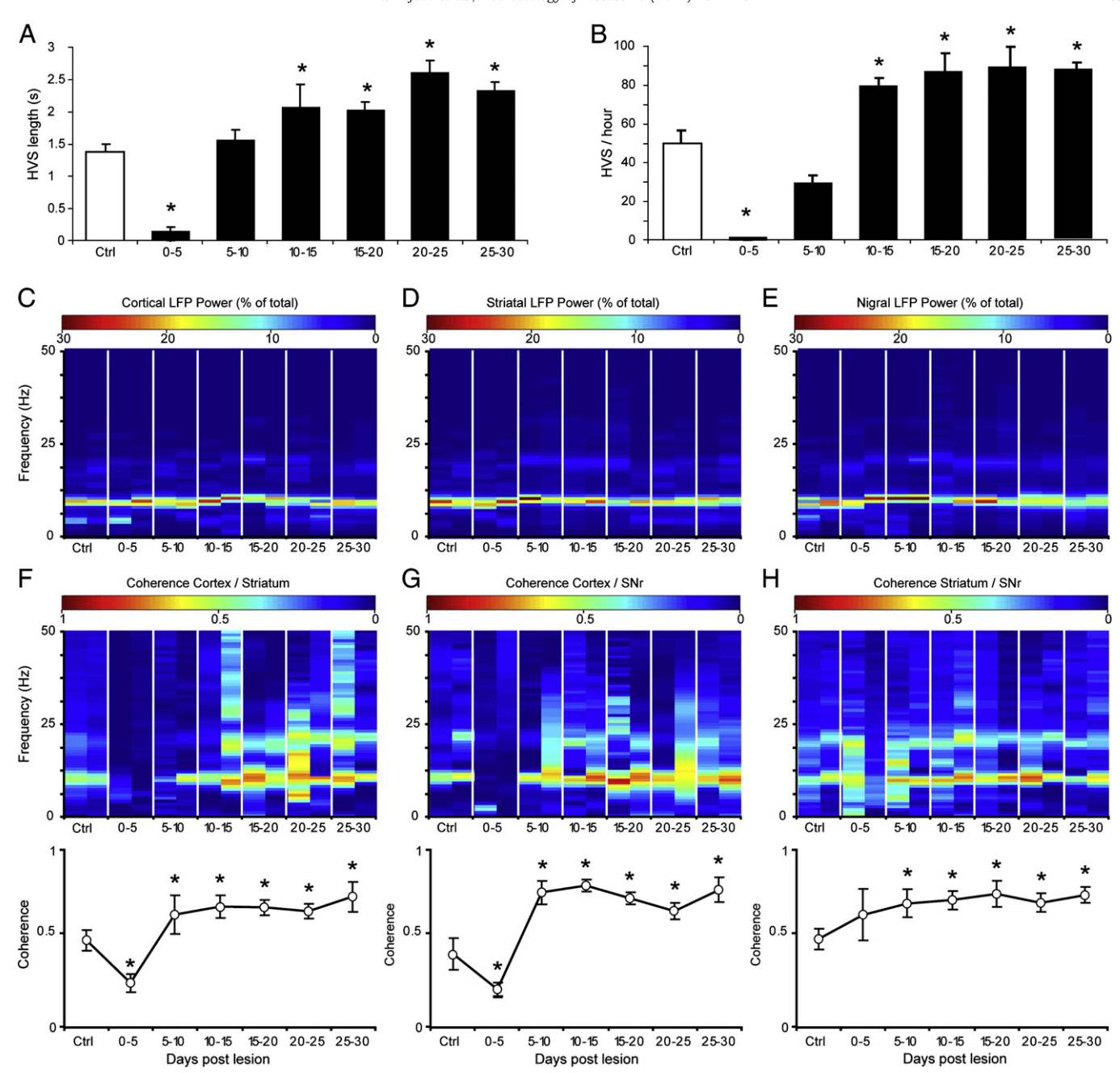


Fig. 4. Evolution of HVS features after nigrostriatal lesion. A. Mean duration of HVS. B. Mean number of HVS per hour of resting behavioral state. Asterisk (*) indicates a significant difference from control condition (one way ANOVA, post hoc: Bonferroni test with p = 0.05). C-E: Power spectral density of the LFP in the cortex (C), striatum (D) and SNr (E). For each 5 day time intervals, 2 examples are displayed with color scaled relative power. F-H: Coherence between pairs of structures. Columns present examples (top) and frequency band averages (bottom) for cortex vs. striatum (F), striatum vs. SNr (G) and cortex vs. SNr (H). Plain line: mean coherence in the alpha band 5–13 Hz, For each time step of 5 days, 2 examples are displayed with color scaled coherence. For averaging plots an asterisk (*) indicates a significant difference from control condition (one way ANOVA, post hoc: Bonferroni test with p = 0.05).

rhythmically entrained neurons were 65% in cortex, 60% in striatum and 58% in the SNr. Following 6-OHDA lesion, these values were significantly increased in cortical and nigral neurons from [5-10] to [25-30] (chi-square test, p<0.05 in all cases), whereas the small overall increase in striatal population was not significant (chi-square test, p>0.05 in all cases).

In control conditions, temporal organization of the structure followed the principle of a top-down activation with cortex preceding striatum and SNr, in that order (Fig. 6). Temporal sequence of neuronal activation perfectly reflected this sequence (Figs. 6 B, E and H) such that cortical neuron firing peaked early $(-5.8 \pm 4.2 \text{ ms}, \text{SEM})$ and preceded striatal peak $(3.2 \pm 3.9 \text{ ms})$ that in turn preceded SNr peak $(40.5 \pm 4.8 \text{ ms})$. After neurotoxin injection, dopaminergic

depletion had no effect on cortical and striatal peak times (Kruskal-Wallis test: p<0.05 for both populations) whereas it did dramatically upset SNr firing organization (Fig. 6G). From [5–10] on, the preferred phase of SNr neurons was significantly advanced and its delay kept on shortening to settle around 10 ms for time periods [15–20], [20–25] and [25–30] (Kruskal–Wallis test: p<0.05 and Dunn's post hoc: p<0.05 for each time range). To test whether a modification of the oscillation period was not the cause for the shortening of SNr activation delay we performed a phase analysis as exemplified in Fig. 6D. As expected following lesion the preferred phase for cortical and striatal neuron remained stable (Watson U2 test, p>0.05 for each comparison control vs [time]) whereas SNr neurons displayed a shift in phase similar to that observed in the time domain (Figs. 6C F and I).

C. Dejean et al. / Neurobiology of Disease 46 (2012) 402-413

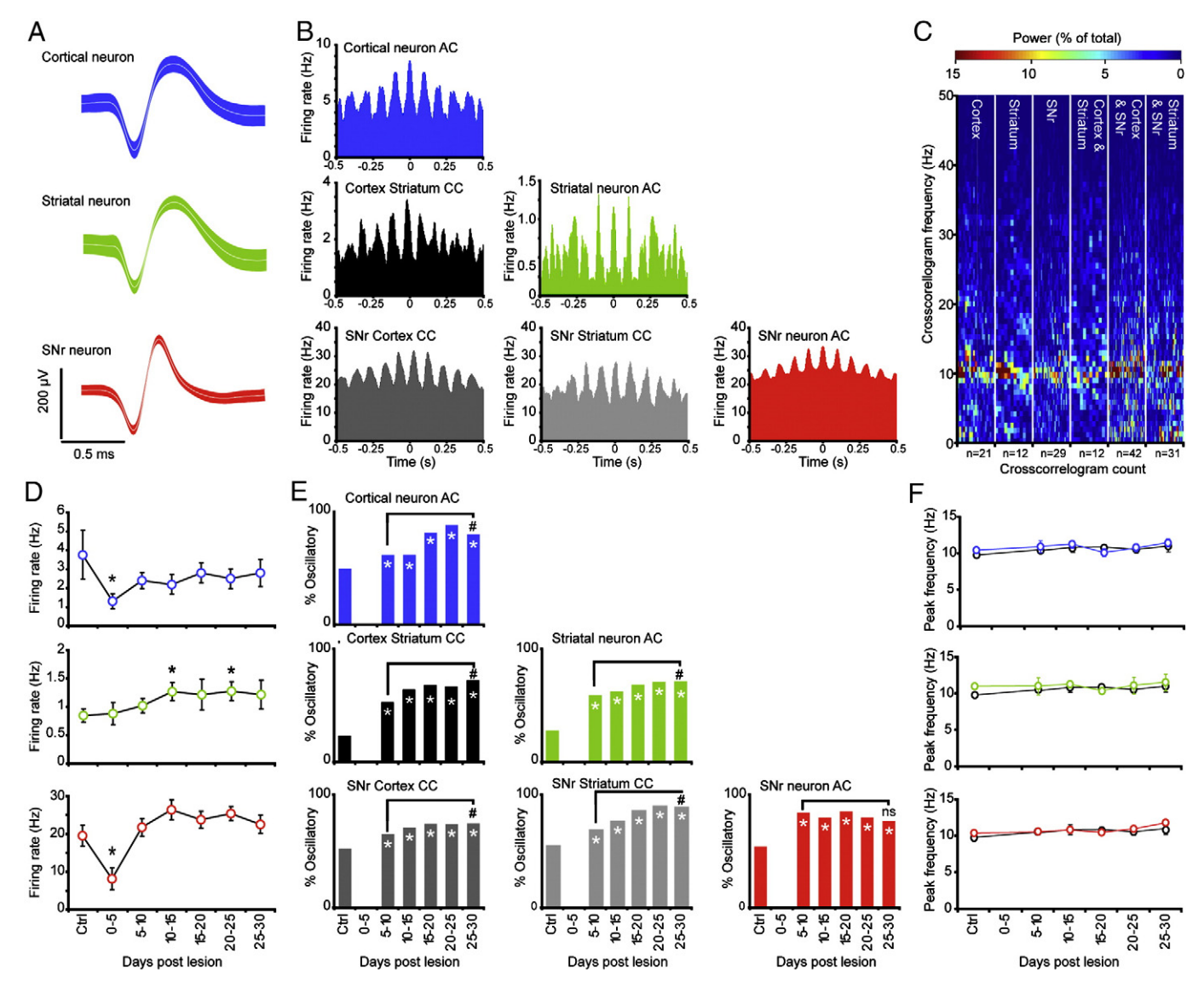


Fig. 5. Single neuron activity. A. Average waveforms for 3 neurons simultaneously recorded in control condition. From top to bottom: cortex, striatum and SNR. B. Crosscorrelation matrix for the 3 neurons shown in (A). The color plot on the diagonal displays autocorrelograms (AC) while the other grayscale plots represent crosscorrelograms for 2 different spike trains (CC). C. Power spectral density of all crosscorrelation functions in control conditions. The relative power is plotted by means of a color scale. D. Evolution of neuron firing rates during HVS after dopaminergic depletion. An asterisk indicates a significant difference with control condition (one way ANOVA, post hoc: Bonferroni test with p = 0.05). E. Time evolving percentage of oscillatory crosscorrelograms (CCs). Color code is the same as for (B). An asterisk indicates a significant difference with control condition (chi square test, p < 0.05). A hash sign represents a significant difference between initial and final periods post lesion. Ns: non significant. F. Evolution of peak frequency in ACs and cortical LFPs. From top to bottom: cortex, striatum and SNr. Evolving AC frequencies did never differ from that in control condition nor that in cortical LFPs for the same time step.

This phase change was detected as soon as [5-10] (Watson U2 test, p<0.05).

Discussion

In this work, we studied the 30 day time-course of the effect of 6-OHDA lesion on the cortex–BG network during HVS. Our results reveal that early changes following intracranial 6-OHDA injection might reflect inflammatory phenomena rather than being specifically dependent on dopamine depletion. We also show that an increase in oscillatory synchronization occurs very soon after the lesion and keeps developing until day 25. We also evidence here a progressive shortening of SNr response delay to cortical activation. The evolution of SNr delay shortening closely reflects the decrease in self-induced locomotion whereas the time course of synchronous oscillations is de-correlated with the observed motor symptoms.

Early physiological changes

Acute DA system blockade is well known to impair locomotion and can reduce motor cortex activity as shown with receptor antagonists (Parr-Brownlie and Hyland, 2005). This decrease could in turn be responsible for SNr cells drop in firing rate. Interestingly the time course of the different behavioral and electrophysiological alterations is not correlated with the kinetics of SNc dopaminergic cell loss which conversely keeps on developing. Therefore early changes observed here are unlikely to derive only from the dopaminergic neuron loss or depletion of this monoamine in the brain. Most of this discrepancy relies on the drastic and transient upset of electrophysiological and behavioral parameters observed within the first five days following the lesion. Since our animal displayed signs of distress (posture, fur) classically associated with sickness behavior we hypothesize that those changes could be due not only to the lesion itself but also to collateral inflammation phenomena. This is supported by findings

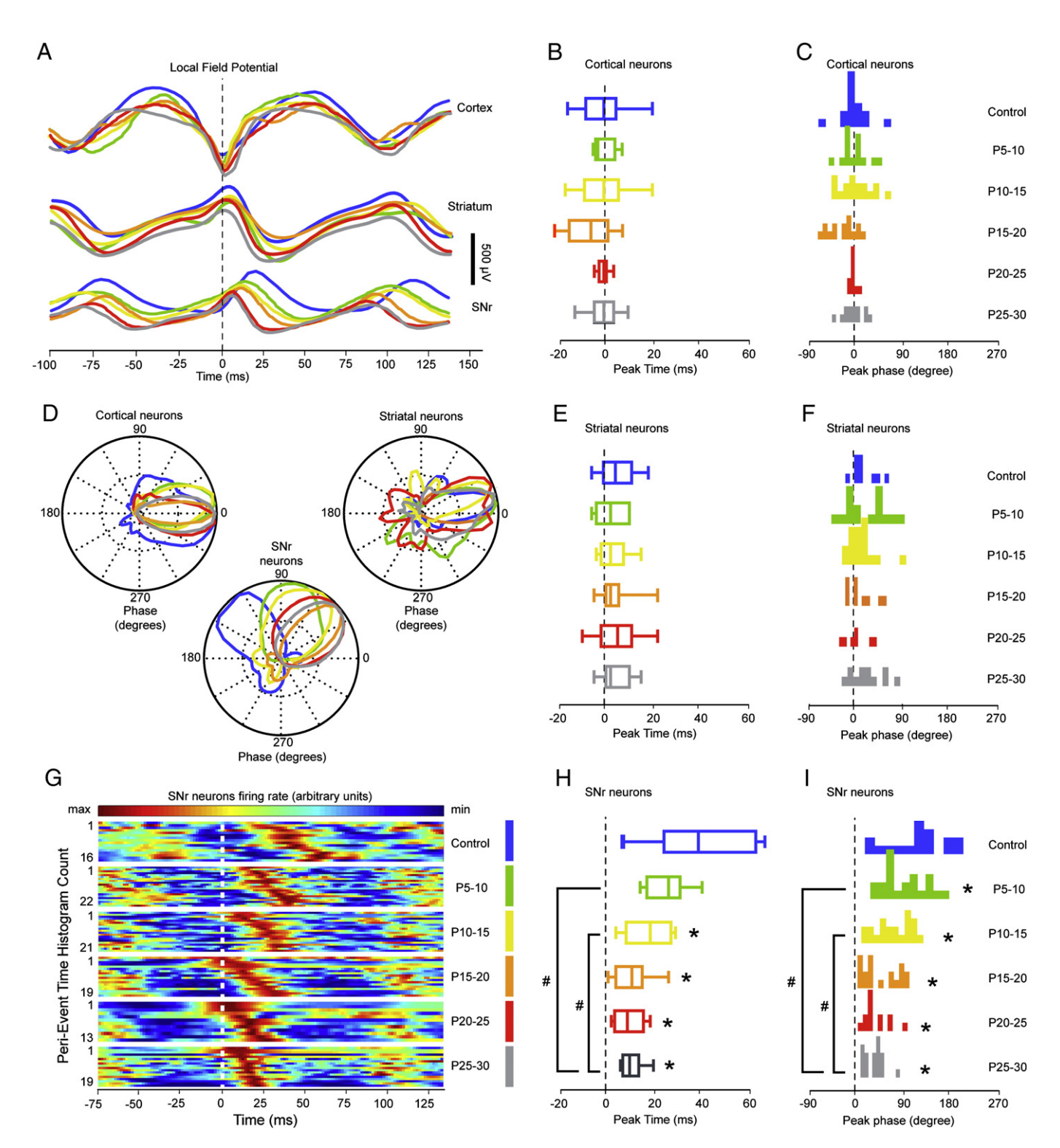


Fig. 6. Temporal organization. A. Local field potentials (LFP) recorded in cortex (top) striatum (middle) and SNr (bottom) triggered on cortical LFP troughs (dotted line) and averaged. The different colors represent LFPs recorded at different time steps pre and post lesion: blue: control, green: 5–10 days post lesion, yellow: 10–15, orange: 15–20, red: 20–25, gray: 25–30. B–C. Distribution of the peak time (B) and phase (C) of cortical neuron discharge triggered by cortical LFP troughs. D. Peristimulus Phase Histograms of single neuron discharge triggered by cortical LFP troughs (zero phase). The polar histogram display examples of normalized instantaneous firing rates of neurons recorded at different stages pre and post lesion. Maximum and minimum diameters respectively represent maximum and minimum firing rates. E–F. Distribution of the peak time (E) and phase (F) of striatal neuron discharge triggered by cortical LFP troughs. Normalized instantaneous firing rates of neurons are plotted as function of time (bin = 2 ms) and color (top color scale). Neurons in each time step are sorted according to their peak time. H–I. Distribution of the peak time (H) and phase (I) of SNr neuron discharge triggered by cortical LFP troughs. An asterisk (*) indicates a significant difference in the distributions of peak times or peak phase compared to control condition. A hash sign (#) represents a significant difference between the final period and other periods post lesion (peak time: Kruskal–Wallis one way ANOVA on ranks followed by a Dunn's *post hoc*, p<0.05, peak phase: Watson U2 test, p<0.05).

showing neuroinflammation in the nigrostriatal pathway following 6-OHDA lesion (Cicchetti et al., 2002). This finding appeal for caution when trying to assess the effect of immediate dopamine depletion in chronic lesion models: the time frame of the study represents a crucial factor to be taken into account when drawing any conclusions.

Immediate and progressive increase in cortex–basal ganglia synchronization after 6-OHDA lesion

Confirming the results of our previous study (Dejean et al., 2008) coherence and correlation analyses revealed a general increase of synchronization in the cortex-BG network after dopamine depletion. This is consistent with the large piece of literature reporting synchronous oscillations in Parkinsonian patients as well as animal models of the disease (Belluscio et al., 2003; Bergman et al., 1994; Brown et al., 2001; Costa et al., 2006; Raz et al., 2001; Sharott et al., 2005). Our multisite-evolutive approach reveals that, taken apart early [0–5] changes, this increase appears soon after the lesion during the [5–10] period. Moreover this increase concerns the entire cortex–striatum-SNr network. This phenomenon is also concurrent with the time when most of dopaminergic neurons have been lost. Therefore dopamine depletion seems to have a direct impact on the network rhythmic activity in line with previous pharmacological studies using dopaminergic agents chronically while recording electrocorticogram in rats (Costa et al., 2006; Deransart et al., 2001; Deransart et al., 2000; Sebban et al., 1999). Despite our dual evolutivemultisite approach it has not been possible to point at any specific part of the cortico-striato-nigral network that could be the cradle of oscillatory impairments. It is still possible that the answer to this question remains to be found in the very early stages following the toxin injection. However inflammatory processes evidenced during this period is a major analytic interference when trying to tackle this issue. An alternative hypothesis is that it results form a drastic change in the network dynamic properties as we predicted from previous theoretical work (Leblois et al, 2006).

Further inspection along the temporal axis reveals that synchronization processes keep strengthening until [15–20] when at that point coherence, the number and length of HVS as well as neuronal oscillations stabilize until completion of the experiment. In line with a recent study focusing on beta oscillations (Mallet et al., 2008), this sustained increase suggests that evolutive phenomena might promote oscillatory firing in the network on top of the simple absence of dopamine. Indeed long-term anatomical and functional rearrangements have been shown to take place in the striatum of 6-OHDA-treated rats (Day et al., 2006; Kreitzer and Malenka, 2007). If the lack of dopamine alone is enough to reinforce cortex–BG oscillations (Degos et al., 2009) it also triggers those plastic changes that could reinforce their presence on a long-term basis.

Progressive shortening of top-down signal transmission

Recent works have shown that SNr neuron response to cortical electrical stimulation is altered after dopamine antagonists injection (Degos et al., 2005) and hyperdirect pathway response is further exacerbated in a chronic model of Parkinson's disease (Belluscio et al., 2007). In our present and previous studies (Dejean et al., 2008) we have shown that a comparable phenomenon is also present during HVS after 6-OHDA lesion as SNr neurons response to descending cortical inputs is shortened and falls in the time range of hyperdirect mediated response. The present study extends those results by showing that this effect is taking place very progressively after the toxin injection. SNr peak firing time start drifting toward smaller delays at [10–15] and peak phase decreases as soon as [5–10]. It stabilizes at [15–20] around 10 ms which correspond to the range of hyperdirect

pathway-induced excitation (Kolomiets et al., 2003; Maurice et al., 1999; Nambu et al., 2000). Conversely the cortical and striatal peak delays or phases did not present any change. The changes in the SNr have been attributed to a joint increase of responsiveness in the indirect pathway and decrease in that of the direct pathway (Belluscio et al., 2007; Degos et al., 2005; Dejean et al., 2008; Mallet et al., 2006). Subsequent weakening of direct pathway-mediated inhibition on the SNr might in return give way to a greater expression of fast hyperdirect pathway-mediated excitatory inputs. Together with evidence that 6-OHDA lesion enhances the magnitude of SNr neuron response to cortical electrical stimulation (Belluscio et al., 2007) the shortening of SNr response observed here might reflects an enhancement of its recruitment by cortex-imposed HVS rhythm.

Interestingly the kinetics of these changes in SNr firing behavior was slower than that of dopamine cell loss. Contrasting with the gradual decrease in SNr delay activation, dopamine cell loss was already severe as soon as [5-10] in line with previous studies (Chalon et al., 1999; Vila et al., 2000; Zuch et al., 2000). Alteration of SNr neuron firing behavior could be well due to changes in the dendritic dopamine release in this area. However because of this temporal discrepancy dopamine depletion cannot account directly for the complete phenomenon. Instead it is possible that cortico-nigral fibers become overactive or that plastic changes occur in the SNr itself. Finally SNr response enhancement could result from plastic modifications that occur after dopamine starts lacking. Elimination of number of cortico-striatal synapses in the indirect pathway (Day et al., 2006) might bridle late excitatory inputs on the SNr and therefore enhance the contrast between activity of the different BG pathways in favor of fast hyperdirect excitatory inputs. The progressive anatomical and functional modifications of BG circuitry could help reinforcing synchronized oscillatory activity in BG outputs and throughout the whole cortex-BG. Together these arguments can account for oscillations to keep increasing several days after dopamine loss has reached its maximum and might also explain why animals chronically depleted in dopamine always present oscillations of greater magnitude (Degos et al., 2009; Mallet et al., 2008; Sharott et al., 2005) than that of animals treated acutely (Dejean et al., 2009; Sebban et al., 1999).

Locomotor impairment correlates with late cerebral changes

The appearance of self-induced locomotion impairment is delayed by no less than 10 days compared to over-synchronization. Temporal decorrelation between oscillations and the appearance of the first symptoms has also been observed in the monkey with a progressive dopaminergic neuron degeneration protocol (Leblois et al., 2007). Importantly both studies show that exacerbated oscillations are neither a necessary nor a sufficient condition to trigger motor impairment. In fact kinetics of oscillatory activity might rather reflect the level of dopamine cells loss in the SNc. This is in line with studies in PD patients showing that oscillations are acutely reduced by dopaminergic therapy (Heimer et al., 2006; Weinberger et al., 2006). Unlike prediction of classic models of PD pathophysiology, the neuronal average firing rates did not show any particular modification as symptoms appear with time. Modifications at the cellular level seem to involve changes in firing dynamics rather than average activity. Indeed the gradual advance of SNr response reflects the slower kinetics of motor impairment. The shortening of spike processing in the BG could be at the origin of akinetic motor symptoms observed in PD. Very recently, alterations in temporal spiking layout have been reported in other models of PD in the monkey (Leblois et al., 2006) and rat (Belluscio et al., 2007; Degos et al., 2005). Together with these studies, our results emphasize that dynamic features of signal processing are crucial in BG physiology and that the alteration of BG ability to process cortical signal seems to be more important in the development of symptoms than the reinforcement of oscillations.

Acknowledgment

The authors want to thank Sandra Dovero and Laura Cardoit for histology as well as Paul Girardeau for help with the experiments. This work was supported by the Centre National de la Recherche Scientifique, the Franco-Israélien de Neurophysiologie et Neurophysique des Systèmes, Bordeaux and the Fondation de France. CD was funded by the Association France Parkinson and the Boehringer-Ingelheim Fonds.

References

- Bartho, P., et al., 2004. Characterization of neocortical principal cells and interneurons by network interactions and extracellular features. J. Neurophysiol. 92, 600–608.
- Belluscio, M.A., et al., 2003. Spreading of slow cortical rhythms to the basal ganglia output nuclei in rats with nigrostriatal lesions. Eur. J. Neurosci. 17, 1046–1052.
- Belluscio, M.A., et al., 2007. Striatal dysfunction increases basal ganglia output during motor cortex activation in parkinsonian rats. Eur. J. Neurosci. 25, 2791–2804.
- Bergman, H., et al., 1994. The primate subthalamic nucleus. II. Neuronal activity in the MPTP model of parkinsonism. J. Neurophysiol. 72, 507–520.
- Berke, J.D., et al., 2004. Oscillatory entrainment of striatal neurons in freely moving rats. Neuron 43, 883–896.
- Bezard, E., et al., 2001. Relationship between the appearance of symptoms and the level of nigrostriatal degeneration in a progressive MPTP-lesioned macaque model of Parkinson's disease. J. Neurosci. 21, 6853–6861.
- Boraud, T., et al., 2005. Oscillations in the basal banglia: the good, the bad and the unexpected. In: Bolam, J.P., et al. (Ed.), The Basal Ganglia VIII. Springer, pp. 3–24.
- Brown, P., et al., 2001. Dopamine dependency of oscillations between subthalamic nucleus and pallidum in Parkinson's disease. J. Neurosci. 21, 1033–1038.
- Chalon, S., et al., 1999. Time course of changes in striatal dopamine transporters and D2 receptors with specific iodinated markers in a rat model of Parkinson's disease. Synapse 31, 1–6.
- Chen, M.T., Morales, M., Woodward, D.J., Hoffer, B.J., Janak, P.H., 2001. In vivo extracellular recording of striatal neurons in the awake rat following unilateral 6-hydroxydopamine lesions. Exp. Neurol. 171, 72–83.
- Cicchetti, F., et al., 2002. Neuroinflammation of the nigrostriatal pathway during progressive 6-OHDA dopamine degeneration in rats monitored by immunohistochemistry and PET imaging. Eur. J. Neurosci. 15, 991–998.
- Costa, R.M., et al., 2006. Rapid alterations in corticostriatal ensemble coordination during acute dopamine-dependent motor dysfunction. Neuron 52, 359–369.
- Day, M., et al., 2006. Selective elimination of glutamatergic synapses on striatopallidal neurons in Parkinson disease models. Nat. Neurosci. 9, 251–259.
- Degos, B., et al., 2005. Neuroleptic-induced catalepsy: electrophysiological mechanisms of functional recovery induced by high-frequency stimulation of the subthalamic nucleus. J. Neurosci. 25, 7687–7696.
- Degos, B., et al., 2009. Chronic but not acute dopaminergic transmission interruption promotes a progressive increase in cortical beta frequency synchronization: relationships to vigilance state and akinesia. Cereb. Cortex 19, 1616–1630.
- Dejean, C., et al., 2007. Synchronous high-voltage spindles in the cortex-basal ganglia network of awake and unrestrained rats. Eur. J. Neurosci. 25, 772–784.
- Dejean, C., et al., 2008. Dynamic changes in the cortex-basal ganglia network after dopamine depletion in the rat. J. Neurophysiol. 100, 385–396.
- Dejean, C., et al., 2009. Cortical effects of subthalamic stimulation correlate with behavioral recovery from dopamine antagonist induced akinesia. Cereb. Cortex 19, 1055–1063.
- Deransart, C., et al., 2000. Dopamine in the striatum modulates seizures in a genetic model of absence epilepsy in the rat. Neuroscience 100, 335–344.
- Deransart, C., et al., 2001. Inhibition of the substantia nigra suppresses absences and clonic seizures in audiogenic rats, but not tonic seizures: evidence for seizure specificity of the nigral control. Neuroscience 105, 203–211.
- Deransart, C., et al., 2003. Single-unit analysis of substantia nigra pars reticulata neurons in freely behaving rats with genetic absence epilepsy. Epilepsia 44, 1513–1520.
- Dunnett, S.B., 1983. Motor function(s) of the nigrostriatal dopamine system: studies of lesions and behavior. In: Dunnett, S.B., et al. (Ed.), Dopamine. Elsevier, Amsterdam, pp. 237–254.
- Eusebio, A., Brown, P., 2007. Oscillatory activity in the basal ganglia. Parkinsonism Relat. Disord. 13 (Suppl 3), S434–S436.
- Fisher, N.I., 1993. Statistical Analysis of Circular Data. Cambridge University Press. Graybiel, A.M., et al., 1994. The basal ganglia and adaptive motor control. Science 265, 1826–1831.
- Hammond, C., et al., 2007. Pathological synchronization in Parkinson's disease: networks, models and treatments. Trends Neurosci. 30, 357–364.
- Heimer, G., et al., 2006. Dopamine replacement therapy does not restore the full spectrum of normal pallidal activity in the 1-methyl-4-phenyl-1,2,3,6-tetra-hydropyridine primate model of Parkinsonism. J. Neurosci. 26, 8101–8114.

- Hutchison, W.D., et al., 2004. Neuronal oscillations in the basal ganglia and movement disorders: evidence from whole animal and human recordings. J. Neurosci. 24, 9240–9243.
- Hyland, B.I., et al., 2002. Firing modes of midbrain dopamine cells in the freely moving rat. Neuroscience 114, 475–492.
- Kandel, A., Buzsáki, G., 1997. Cellular-synaptic generation of sleep spindles, spike-and-wave discharges, and evoked thalamocortical responses in the neocortex of the rat. I. Neurosci. 17. 6783–6797.
- Kish, L.J., Palmer, M.R., Gerhardt, G.A., 1999. Multiple single-unit recordings in the striatum of freely moving animals: effects of apomorphine and p-amphetamine in normal and unilateral 6-hydroxydopamine-lesioned rats. Brain Res. 833, 58–70.
- Klausberger, T., et al., 2003. Brain-state- and cell-type-specific firing of hippocampal interneurons in vivo. Nature 421, 844-848.
- Kolomiets, B.P., et al., 2003. Basal ganglia and processing of cortical information: functional interactions between trans-striatal and trans-subthalamic circuits in the substantia nigra pars reticulata. Neuroscience 117, 931–938.
- Kravitz, A.V., et al., 2010. Regulation of parkinsonian motor behaviours by optogenetic control of basal ganglia circuitry. Nature 466, 622–626.
- Kreitzer, A.C., Malenka, R.C., 2007. Endocannabinoid-mediated rescue of striatal LTD and motor deficits in Parkinson's disease models. Nature 445, 643–647.
- Kunikowska, G., Jenner, P., 2001. 6-Hydroxydopamine-lesioning of the nigrostriatal pathway in rats alters basal ganglia mRNA for copper, zinc- and manganese-superoxide dismutase, but not glutathione peroxidase. Brain Res. 922, 51–64.
- Leblois, A., et al., 2006. Temporal and spatial alterations in GPi neuronal encoding might contribute to slow down movement in Parkinsonian monkeys. Eur. J. Neurosci. 24, 1201–1208.
- Leblois, A., et al., 2007. Late emergence of synchronized oscillatory activity in the pallidum during progressive Parkinsonism. Eur. J. Neurosci. 26, 1701–1713.
- Magill, P.J., et al., 2005. Coherent spike-wave activity in the cortex and subthalamic nucleus of the freely moving rat. Neuroscience 132, 659–664.
- Mallet, N., et al., 2006. Cortical inputs and GABA interneurons imbalance projection neurons in the striatum of parkinsonian rats. J. Neurosci. 26, 3875–3884.
- Mallet, N., et al., 2008. Disrupted dopamine transmission and the emergence of exaggerated beta oscillations in subthalamic nucleus and cerebral cortex. J. Neurosci. 28, 4795–4806.
- Maurice, N., et al., 1999. Relationships between the prefrontal cortex and the basal ganglia in the rat: physiology of the cortico-nigral circuits. J. Neurosci. 19, 4674–4681.
- Nambu, A., et al., 2000. Excitatory cortical inputs to pallidal neurons via the subthalamic nucleus in the monkey. J. Neurophysiol. 84, 289–300.
- Olsson, M., et al., 1995. Forelimb akinesia in the rat Parkinson model: differential effects of dopamine agonist and nigral transplants as assessed by a new stepping test. J. Neurosci. 15, 3863–3875.
- Parr-Brownlie, L.C., Hyland, B.I., 2005. Bradykinesia induced by dopamine D2 receptor blockade is associated with reduced motor cortex activity in the rat. J. Neurosci. 25, 5700–5709.
- Paxinos, G., Watson, C., 1998. The Rat Brain in Stereotaxic Coordinates. Academic Press, New York.
- Polack, P.O., et al., 2007. Deep layer somatosensory cortical neurons initiate spikeand-wave discharges in a genetic model of absence seizures. J. Neurosci. 27, 6590–6599.
- Raz, A., et al., 2001. Activity of pallidal and striatal tonically active neurons is correlated in MPTP-treated monkeys but not in normal monkeys. J. Neurosci. 21 (1–5), RC128.
- Sebban, C., et al., 1999. Changes in EEG spectral power in the prefrontal cortex of conscious rats elicited by drugs interacting with dopaminergic and noradrenergic transmission. Br. J. Pharmacol. 128, 1045–1054.
- Sharott, A., et al., 2005. Dopamine depletion increases the power and coherence of beta-oscillations in the cerebral cortex and subthalamic nucleus of the awake rat. Eur. J. Neurosci. 21, 1413–1422.
- Shaw, F.Z., 2004. Is spontaneous high-voltage rhythmic spike discharge in Long Evans rats an absence-like seizure activity? J. Neurophysiol. 91, 63–77.
- Slaght, S.J., et al., 2004. On the activity of the corticostriatal networks during spike-and-wave discharges in a genetic model of absence epilepsy. J. Neurosci. 24, 6816–6825.
- Steiner, H., Kitai, S.T., 2001. Unilateral striatal dopamine depletion: time-dependent effects on cortical function and behavioural correlates. Eur. J. Neurosci. 14, 1390–1404.
- Vergnes, M., et al., 1990. Mapping of spontaneous spike and wave discharges in Wistar rats with genetic generalized non-convulsive epilepsy. Brain Res. 523, 87–91.
- Vila, M., et al., 2000. Evolution of changes in neuronal activity in the subthalamic nucleus of rats with unilateral lesion of the substantia nigra assessed by metabolic and electrophysiological measurements. Eur. J. Neurosci. 12, 337–344.
- Weinberger, M., et al., 2006. Beta oscillatory activity in the subthalamic nucleus and its relation to dopaminergic response in Parkinson's disease. J. Neurophysiol. 96, 3248–3256.
- Windels, F., Kiyatkin, E.A., 2006. General anesthesia as a factor affecting impulse activity and neuronal responses to putative neurotransmitters. Brain Res. 1086, 104–116.
- Zuch, C.L., et al., 2000. Time course of degenerative alterations in nigral dopaminergic neurons following a 6-hydroxydopamine lesion. J. Comp. Neurol. 427, 440–454.